

On the Natural Convection in the Columnar to Equiaxed Transition in Directionally Solidified Aluminum-based Binary and Multicomponent Alloys

Carlos Henrique Ursolino Gomes^a, Rafael Hideo Lopes Kikuchi^b, André dos Santos Barros^a,

José Nazareno Santos da Silva^b, Maria Adrina Paixão de Sousa da Silva^a,

Antonio Luciano Seabra Moreira^a, Otávio Fernandes Lima da Rocha^{a,b*}

^aInstitute of Technology, Universidade Federal do Pará – UFPA,
Av. Augusto Corrêa, 1, CEP 66075-110, Belém, PA, Brazil

^bInstituto Federal de Educação, Ciência e Tecnologia do Pará – IFPA,
Av. Almirante Barroso, 1155, CEP 66093-020, Belém, PA, Brazil

Received: September 2, 2015; Revised: October 18, 2015

In order to investigate the effect of natural convection in columnar to equiaxed transition (CET), Al-3.0wt.%Cu and Al-3.0wt.%Cu-5.5wt.%Si alloys ingots were obtained during the transient horizontal directional solidification (THDS). Aiming to analyze the effect of superheat in the formation of the macrostructure in ternary Al-Cu-Si alloy, the experiments were conducted with three superheat temperatures above the liquidus temperature of the ternary alloy. A water-cooled solidification experimental device was used. Continuous temperature measurements were made during solidification at different positions in the casting and the data were automatically acquired. Thermal analysis has been applied to determine the thermal parameters such as growth rate (V_L), cooling rate (T_R) and temperature gradient (G_L), whose values have been interrelated with the CET. The observation of the macrostructures has indicated that the resulting thermosolutal convection combined with superheat seem to favor the transition, which did not occur in a single plane, for all ingots obtained, i.e., it has been seen in a range of positions in ingots. The addition of Si element in binary Al-Cu alloy anticipates the CET. A comparison with experimental results for CET occurrence in different growth directions has been carried out.

Keywords: *columnar to equiaxed transition, horizontal directional solidification, thermal parameters, transient conditions, Al-Cu-Si alloys*

1. Introduction

Aluminum casting alloys have properties which are of great industrial interest, such as low density, good corrosion resistance, high thermal and electrical conductivities, good combination of mechanical properties, good workability in machining processes and mechanical forming. Currently, these alloys are produced in various systems and solute contents¹. The literature presents a number of theoretical and experimental, focusing on the macrostructural and microstructural evolution of binary aluminum alloys, however, there are few studies in the literature addressing important families of multicomponent aluminum alloys. In this context, the Al-Cu-Si ternary is a system of particular outstanding properties such as high mechanical strength, low weight and very good fluidity. These qualities make it a good choice for applications in the automotive and aerospace industry. The potential of such alloys has attracted the attention of researchers with a view to investigating the microstructure evolution, and the formation of both macrosegregation and porosity during the solidification process.

Solidification studies can be grouped into two categories: those involving solidification in steady-state heat flow and

those in the unsteady-state regime¹⁻⁵. Investigations of the unsteady-state regime are of prime importance since this class of heat flows encompasses the majority of industrial solidification processes. For the latter, theoretical models and experimental results concerning structural parameters are scarce in the literature. It is known that the vast majority of the studies reported in the literature is intended to analyze the upward solidification process which is completely stable in view of the liquid movement, i.e., there are no convective currents or neither by temperature differences nor by density differences. This allows experimental analysis and theoretical calculations exempt from this complication, since the heat transfer into the ingot is performed essentially one-dimensional heat conduction^{5,6}.

On the other hand, in the cases of downward and horizontal directional solidification processes there is convection by temperature differences in the liquid^{5,7,8}. During the downward solidification, if the solute rejected causes interdendritic liquid density greater than the nominal liquid, convective motion also occurs by density differences. Moreover, in the horizontal directional solidification the convection in function of the composition gradients in the liquid always occurs⁵.

*e-mail: otavio.rocha@ifpa.edu.br

Another phenomenon is the direction of the gravitational force acting during these solidification processes. Concerning the macrostructural and microstructural analysis, the effects of the gravity direction have been studied with the chill placed mainly on the bottom or top of the mold (upward and downward solidification processes, respectively)^{1-6,9-12}. It is known that there are few published studies on this phenomenon in the case of horizontal direction^{7,8}. The three solid growth directions can be seen schematically in Figure 1.

Establishing correlations between structure and the resulting properties is a complex study that begins with the analysis of different structural aspects. It is also known that the mechanical characteristics of solidified products strongly depend on the macrostructural and microstructural arrangement. On the whole, the macrostructure of cast ingots consists of three different zones: the chill, columnar, and equiaxed zones. The origin of each one has been the subject of intense experimental and theoretical investigation. A more complex structural form is composed of two structural ones, i.e., by columnar to equiaxed transition (CET). The prediction of this transition is of great interest in the programming of mechanical properties of cast products. Published studies suggest that CET is influenced by the following factors: system and composition of the alloy, mold's material and

temperature, superheats, interfacial heat transfer coefficient and convective flow¹⁻¹⁶.

The change of columnar to equiaxed grain structure is a very common occurrence in cast metal products, and numerous mechanisms based on experimental evidence have been proposed for this transition (CET), however, mathematical models to predict this structural transition have had limited success due to its complex solutions to the problem in macro and microscopic levels (heat and mass transfer, nucleation and dendritic growth, respectively)^{6,10-17}. These models excessively simplify the treatment of convection in the liquid and the movement of equiaxed grains. These models have been tested mostly for binary alloys.

A number of experimental investigations have been reported in the literature which suggest that the CET occurs when the solidification thermal parameters such as growth rate (V_L), temperature gradient (G_L) and cooling rate (T_R) reach critical values. The state of the scientific art on CET has been commented in recent works^{7,17}, whose results of these investigations are summarized in Table 1.

2. Experimental Procedure

Experiments were performed with a aluminum-based multicomponent alloy and a binary Al-Cu having as nominal compositions Al-3.0wt%Cu-5.5wt.%Si and Al-3.0wt.%Cu,

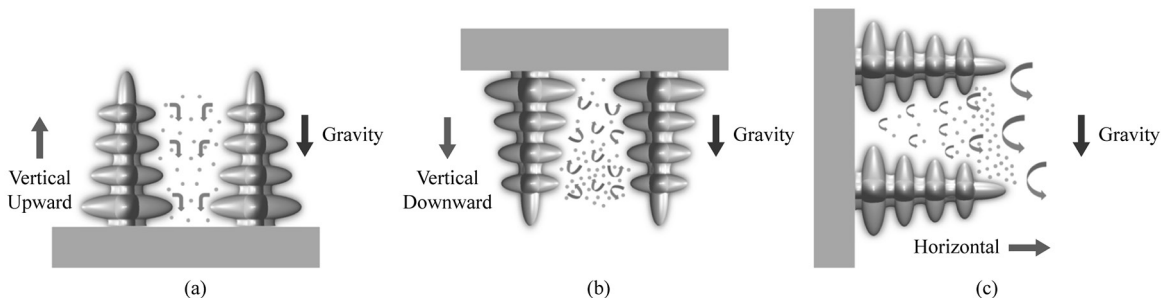


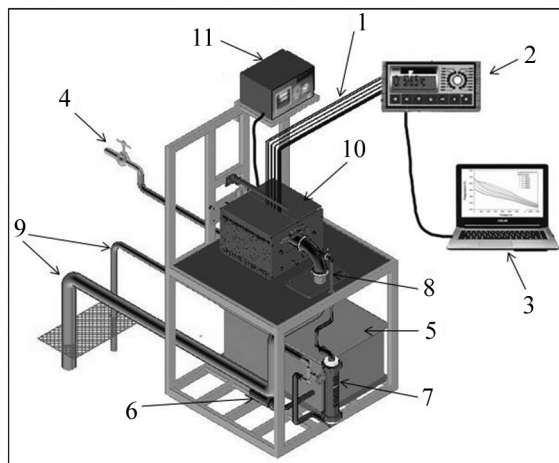
Figure 1. (a) Vertical upward solidification: stable interdendritic liquid (b) Vertical downward solidification: unstable interdendritic liquid (c) Horizontal solidification: unstable interdendritic liquid caused by solutal convection.

Table 1. CET occurrence criteria proposed in the literature.

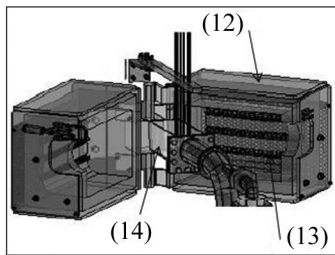
Alloy	Solidification thermal parameter (CET occurrence values)	Directional Solidification	Ref.
Sn-5wt.%Pb Sn-15wt.%Pb	$G_L=0.10$ °C/mm $G_L=0.13$ °C/mm	Upward	Mahapatra & Weinberg ¹⁸
Al-3.0%Cu	0.06 °C/mm	Upward	Ziv & Weinberg ¹⁹
Al-4.5%Cu	$G_L < V_L^{0.64}$	Upward	Suri et al. ²⁰
Pb-Sn	G_L ranging from -0.8 to 1.0 °C/mm	Upward	Ares & Schvezov ²¹
Al-Cu	$T_R=0.2$ K/s	Upward	Siqueira et al. ³
Sn-Pb	$T_R=0.014$ K/s		
Al-Si	$T_R=0.14$ K/s	Upward	Peres et al. ¹
Sn-Pb	$V_L=0.189$ mm/s, $G_L=0.163$ °C/mm and $T_R = 0.030$ K/s	Downward	Spinelli et al. ⁵
Sn-Pb	$V_L=0.09$ mm/s, $G_L=0.37$ °C/mm and $T_R = 0.047$ K/s	Horizontal	Silva et al. ⁸
Al-Si	V_L, G_L and T_R ranging from: 0.19 to 0.26 mm/s, 0.35 to 0.64 K/s and 1.68 to 3.25 K/mm, respectively	Horizontal	Carvalho et al. ⁷
Al-Si-Cu	$T_R = 1.17$ K/s	Upward	Rocha et al. ¹⁷

respectively. The chemical compositions of commercially pure metals that were used to prepare alloy investigated are presented in Table 2.

The horizontal directional solidification (HDS) device used in this study is schematized in Figure 2. It consists of a cooling system comprising of a water pump and flowmeter which ensure water flow 30 LPM. This has allowed to impose both transient growth rate (V_L) and cooling rate (T_R) during solidification. The apparatus also consists of a rectangular mold with heat being extracted only by a water cooled side, providing horizontal directional solidification. A stainless steel mold was used which was 150 mm long, 60 mm wide, 60 mm high and 3 mm thick. The side, top and bottom surfaces were insulated by refractory bricks and heated by electrical heaters to avoid heat losses to the environment. One of the



(a)



(b)

Figure 2. (a) Schematic representation of the horizontal experimental solidification setup: (1) thermocouples, (2) fieldlogger, (3) computer and data acquisition software, (4) feed water, (5) water container, (6) water pump, (7) rotameter, (8) water inlet, (9) water outlet, (10) directional solidification device and (11) temperature controller; (b) view inside of the solidification device: (12) insulating ceramic shielding, (13) electric heaters and (14) rectangular mold (stainless steel mold - inner wall).

side mold part was closed with a 4 mm thick stainless steel mold sheet. Figure 3a shows a schematic drawing of the assembly of the mold and the mold sheet. The alloys were melted in situ, and the lateral electric heaters had their power controlled in order to permit the desired superheat to be achieved. It is noteworthy that the device is monitored by a temperature controller. To start solidification, the electric heaters were disconnected and at the same time the controlled water flow was initiated. In order to analyze the influence of superheat on the macrostructure of the Al-Cu-Si alloy, the initial melt temperatures were standardised at 5%, 10% e 15% above the analyzed alloy liquidus temperature (T_L). The solidification of the alloy Al-3.0wt.% Cu occurred for a superheat of 5%.

It can be seen in Figure 2 that a set of fine K-type thermocouples, sheathed in 1.6 mm outside diameter stainless steel tubes, were inserted in the geometrical centre of the rectangular mould cavity along its length at different positions from the heat-extracting (mould/mould sheet) surface at the bottom of the casting. All the thermocouples were connected by coaxial cables to a data logger interfaced with a computer.

The rectangular ingots obtained for each superheat assumed in this work were sectioned on a midlongitudinal plane, mechanically polished using abrasive papers and etched with

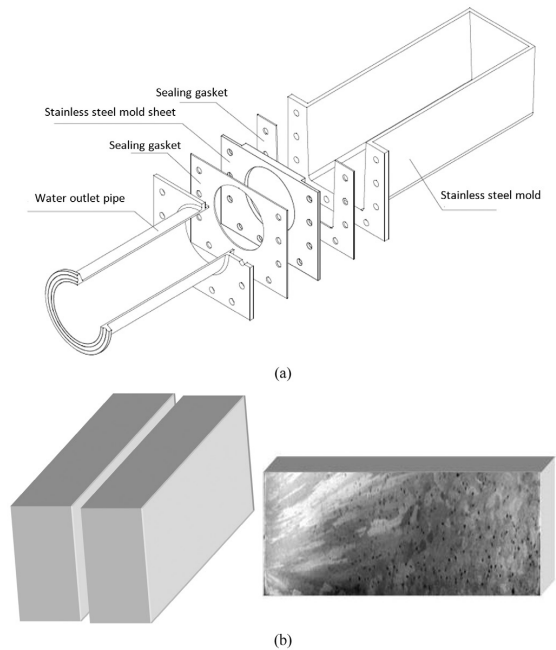


Figure 3. Schematic representation of: (a) assembly of the stainless steel mold and mold sheet set (AISI310); (b) cutting of the ingot for macrostructural revelation.

Table 2. Chemical composition of metals used to prepare the examined alloys.

Metal	Chemical composition (wt.%)							
	Al	Ca	Cu	Fe	Ni	P	S	Si
Al	balance	0.1033	–	0.1827	–	–	–	0.1180
Si	0.0835	–	–	0.2058	0.0159	–	0.0067	balance
Cu	0.0951	–	balance	–	–	0.0450	–	–

an acid solution composed of 70 ml of H₂O, 10 ml of HCl, 15 ml of HNO₃ and 5 ml of HF to reveal the macrostructures as shown schematically in Figure 3b. The chemical attack was conducted to confirm the directionality of solidification, the structural morphology and especially the verification of the columnar to equiaxed transition. The position of the CET was clearly delineated and the distance from the cooled-mold sheet of the casting was measured.

3. Results and Discussion

Experimental cooling curves for thermocouples placed at specific positions into the castings were obtained for the studied alloys in this work, which are shown in Figure 4.

It is known from the literature that the CET is dependent of V_L , G_L and T_R and that during transient solidification these thermal parameters vary with time and position. In this sense, in order to investigate the effect of these parameters on the CET occurrence in analyzed alloys, cooling curves from the Figure 4 were used to determine the displacement of the liquidus isotherm as well as V_L , T_R , and G_L values. A power equation of liquidus isotherm position (P) versus time given by $P = \text{Constant} (t)^n$ (see Figure 5) was obtained for both examined alloys. This has been experimentally

determined from the intersection of corresponding lines to the liquidus temperature (T_L) with the temperature variation curves with time computed for each thermocouple (Figure 4). The derivative of the power function $P = f(t)$ allowed to determine the growth rates. The cooling curves shown in Figure 4 have also been used to determine cooling rates, according to the methodology proposed by Rocha et al.²² and temperature gradients were obtained by the analytical expression $T_R = V_L \cdot G_L^5$. It can be seen in Figure 5 during the THDS of Al-3.0wt.%Cu-5.5wt.%Si alloy that the same experimental laws $P = f(t)$, $V_L = f(P)$, $G_L = f(P)$, and $T_R = f(P)$ were obtained for pouring temperatures 10% and 15% above liquidus temperature. It can be also observed higher values of V_L and T_R for the superheat of 5%. It is noted in Figure 5 that, for the superheat of 5%, the addition of Si element in the formation of Al-Cu-Si alloy has influenced for obtaining higher values of V_L , T_R and G_L , except in positions up to 25 mm, when it was observed higher values of V_L for the Al-3.0wt.%Cu alloy. It is known that when the Si solidify it expands, allowing a better contact at the metal/mold interface, favoring heat transfer coefficient and thus higher growth rates and growth cooling are obtained. On the other hand, thermal conductivity (K), 202.7 W/m.K and 90.7 W/m.K for liquid and solid phases, respectively, and the fusion

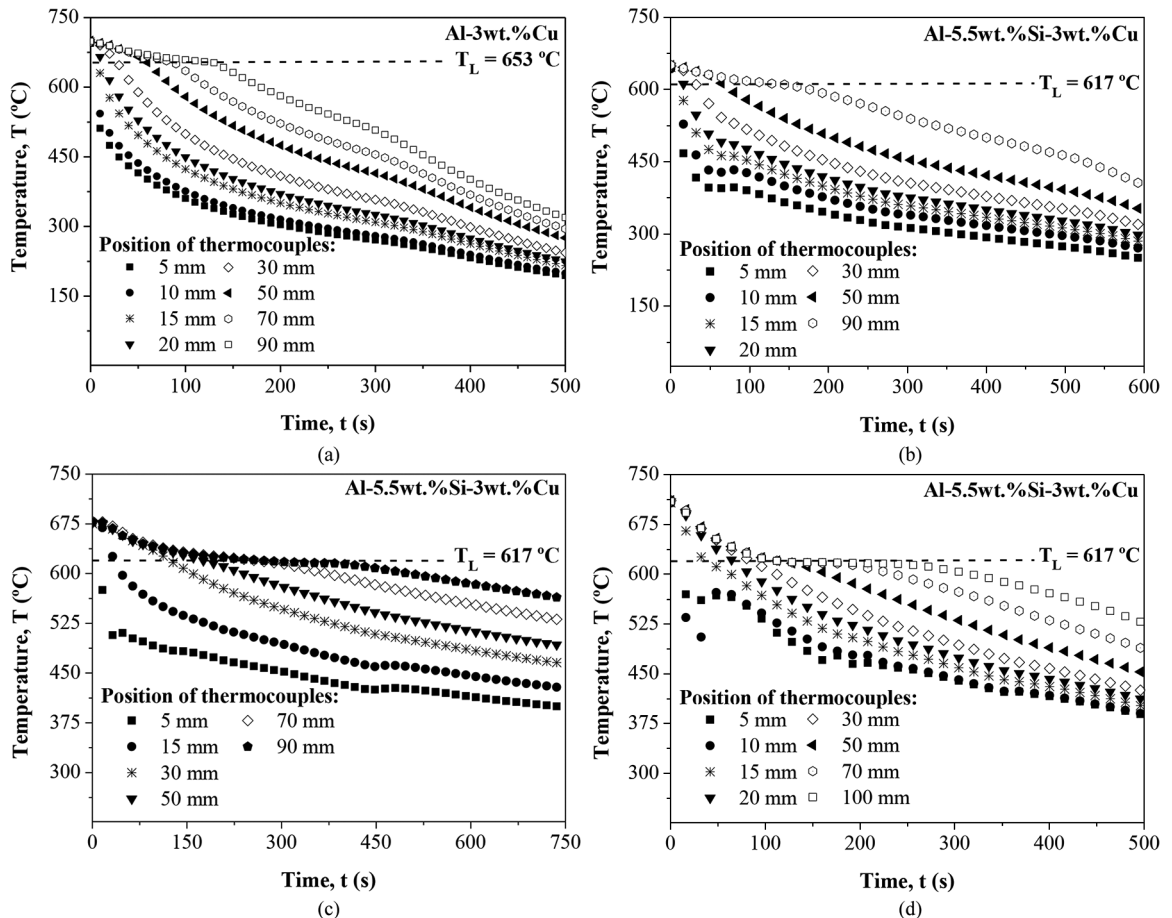


Figure 4. Cooling curves for: (a) Al-3wt.%Cu alloy; (b) Al-3wt.%Cu-5.5wt.%Si alloy with 5% of superheat; (c) Al-3wt.%Cu-5.5wt.%Si alloy with 10% of superheat; (d) Al-3wt.%Cu-5.5wt.%Si alloy with 15% of superheat.

latent heat of the Al-3.0wt.%Cu alloy (ΔH), 382849 J/kg, are higher than the respective values of these properties of the Al-3.0wt.%Cu-5.5wt.%Si alloy, 202.7 W/m.K and 90.7 W/m.K for liquid and solid phases, respectively, and 232100 J/kg, and with the progress of solidification it is possible that the total heat extracted from the metal/mold system is being influenced by these properties, favoring higher V_L values for Al-3.0wt.%Cu alloy from to position from 25 mm, as seen in Figure 5b. Table 3 shows the experimental equations of the solidification thermal parameters obtained during the horizontal directional solidification under the assumed conditions in this work.

Figure 6 shows the macrographs of solidification structures obtained in this study, for the Al-3.0wt.%Cu alloy, solidified under superheat of 5% above liquidus temperature,

and for the Al-3.0wt.%-5.5wt.%Si alloy, solidified 5%, 10% and 15% of superheat. It is observed in all the cases that CET is not sharp. In the case of ternary alloy, it is observed that the macrostructure transition is anticipated for higher superheats. A recent work⁷ has been conducted to analyze the influence of thermal parameters on the CET during horizontal directional solidification of Al-nSi alloys, with "n" equal to 3wt.%, 7wt.% and 9wt.%, and one single superheat of 10% has been assumed for all compositions. As opposed to the present study, the results have showed that the CET was sharp and CET position has occurred for V_L , T_R and G_L in the range between 0.19 to 0.26 mm/s, 0.35 and 0.64 K/s and 1.39 to 4.01 K/mm, however, for any of three alloy compositions examined, the increasing of solute content in Al-Si alloys was not found to affect significantly the

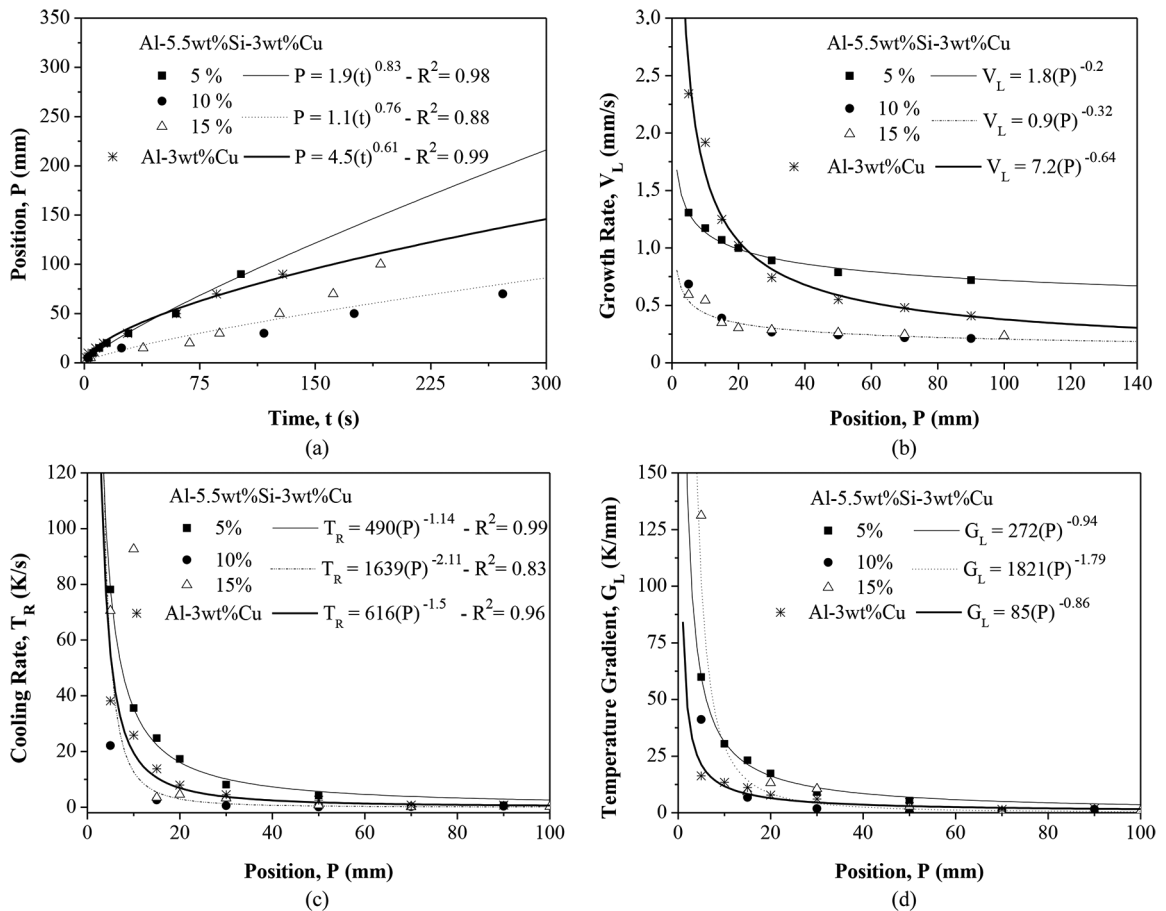


Figure 5. (a) Experimental position of liquidus isotherm from the metal/mold interface as function of time; (b) growth rate as a function of position; (c) cooling rate as a function of position; (d) temperature gradient as a function of position for Al-3wt.%Cu and Al-5.5wt.%Si-3wt.%Cu alloys.

Table 3. Experimental power laws obtained in the present study.

Alloys	Superheat [%]		Experimental power laws		
	5	10	$V_L = 1.8(P)^{-0.20}$	$T_R = 490(P)^{-1.14}$	$G_L = 272(P)^{-0.94}$
Al-3wt.%Cu-5.5wt.%Si	10	$P = 1.1(t)^{0.76}$	$V_L = 0.9(P)^{-0.32}$	$T_R = 1639(P)^{-2.11}$	$G_L = 1821(P)^{-1.79}$
	15				
Al-3wt.%Cu	6	$P = 4.5(t)^{0.61}$	$V_L = 7.2(P)^{-0.64}$	$T_R = 616(P)^{-1.50}$	$G_L = 85(P)^{-0.86}$

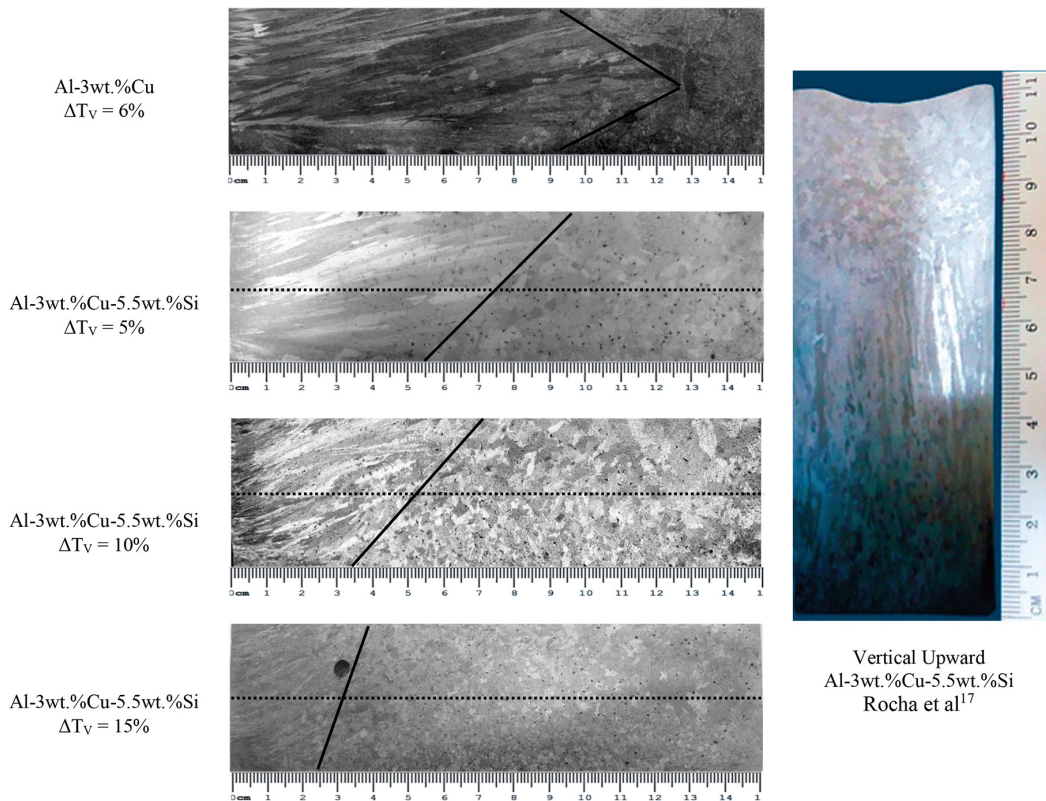


Figure 6. Macrostructures of the Al-3wt.%Cu and Al-3wt.%Cu-5.5wt.%Si alloys.

experimental position of the CET. On the other hand, due to the convective effects caused by horizontal directional solidification, these results⁷ have also shown that the end of the columnar zone was abbreviated as a result of about six times higher thermal gradient than that verified during upward unidirectional solidification of Al-Si alloys¹. More recently, in another investigation on CET occurrence in Al-Cu-Si alloys¹⁷ it was shown that the end of the columnar zone was abbreviated as a result of seven times higher critical cooling rate than that verified for Al-Si alloys¹. It was verified (see Figure 6 for upward solidification) for the Al-3.0wt.%Cu-5.5wt.%Si alloy upward directionally solidified¹⁷ that the CET has occurred in a single plane. Both works have been developed for upward directional solidification (see Table 1).

Concerning the observed characteristics in the macrostructural transition, i.e., sharp and not sharp, respectively, for Al-Si alloys⁷ and Al-3.0wt.%Cu-5.5wt.%Si alloy, the results can be assigned to effect of higher density of Cu alloying element in the composition of ternary alloy as well as due to the solute segregation (Si and Cu) caused at the solidification front which is denser than the liquid overall volume. Therefore, it is possible that both the solute segregation and the effect of gravity acting perpendicularly to solid growth direction cause the decantation of a liquid richer in Cu favoring anticipation of CET in this region.

It is well known that melt convection favors the occurrence of equiaxed grains and that during the transient horizontal directional solidification the effect of thermosolutal convection, when combined with the superheat, seems to prevail for

anticipating of CET. This can be explained by the combined action of both thermal and mechanical convection caused respectively, by superheat and movement of solute at the solidification interface, contributing to the fragmentation of the columnar dendritic branches and, at the same time, promoting the dissipation of superheat increasing the survival of these branches and decreasing the length of the columnar zone. This allowed the CET occurrence for the alloys analyzed, under the conditions assumed in this work in a region with V_L , T_R and G_L varying in a range of values, as shown in the Figures 7-9. The role of addition of Si alloying element in Al-3.0wt.%Cu alloy was also analyzed as indicated in Figure 6. It is noted that Si influences to anticipate the CET. Table 4 shows the experimental thermal parameters associated to the CET position for all alloys investigated in this work. Spinelli et al.⁵ have investigated the effect of melt convection on the columnar to equiaxed transition and microstructure of downward unsteady-state directionally solidified Sn-Pb alloys. According to the authors, in downward solidification conditions, melt convection seems to favor the structural transition. These authors have caused that the melt convection provoked by solute segregation may be promoting pile up of equiaxed grains formed from fractioned dendritic arms, which must stimulate and anticipate the CET occurrence.

The effect of both direction of gravity vector and thermosolutal convection in the transition zone, in microstructural scale, can be seen in macrostructure shown in Figure 10. It is observed the existence of anisotropic and isotropic dendritic morphology, i.e., where both columnar and equiaxed dendrites coexist.

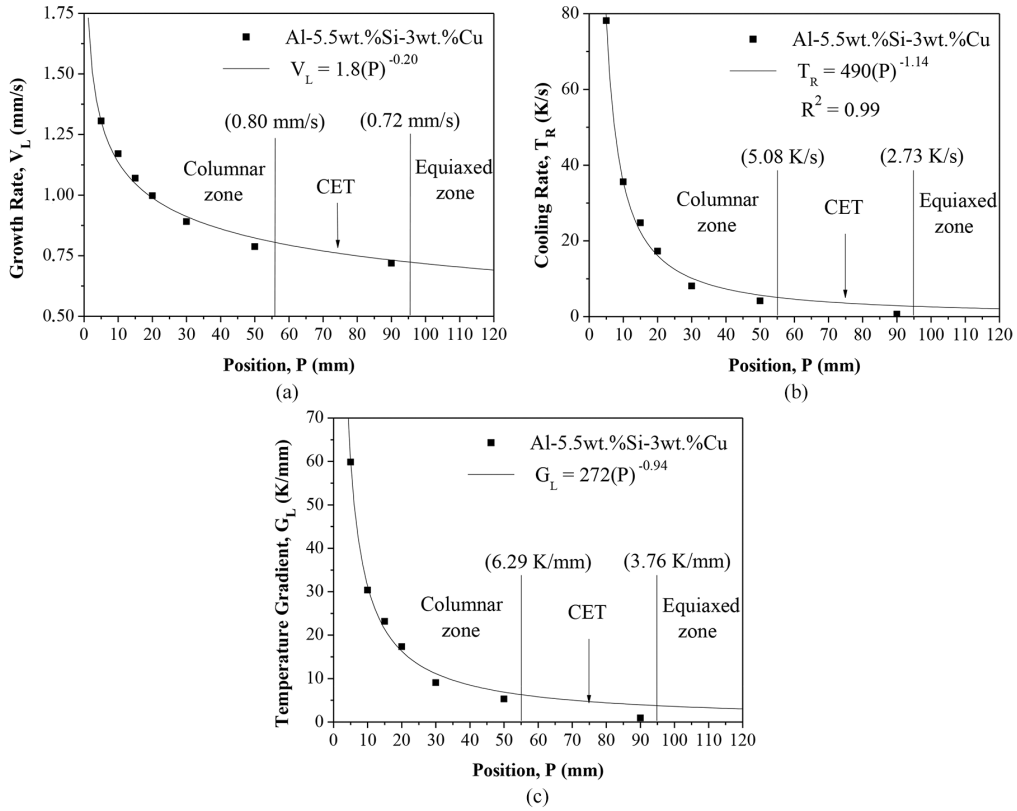


Figure 7. Solidification thermal parameters for Al-3wt.%Cu-5.5wt.%Si alloy with 5% of superheat: (a) $V_L=f(P)$, (b) $T_R=f(P)$ and (c) $G_L=f(P)$.

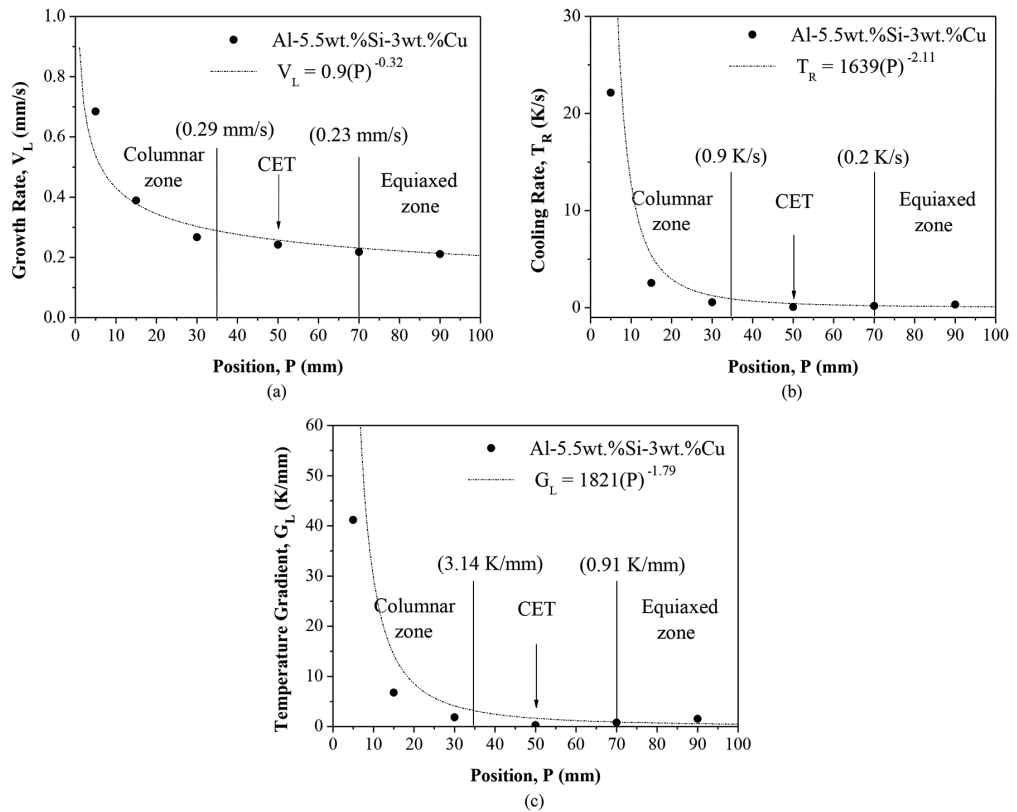


Figure 8. Solidification thermal parameters for Al-3wt.%Cu-5.5wt.%Si alloy with 10% of superheat: (a) $V_L=f(P)$, (b) $T_R=f(P)$ and (c) $G_L=f(P)$.

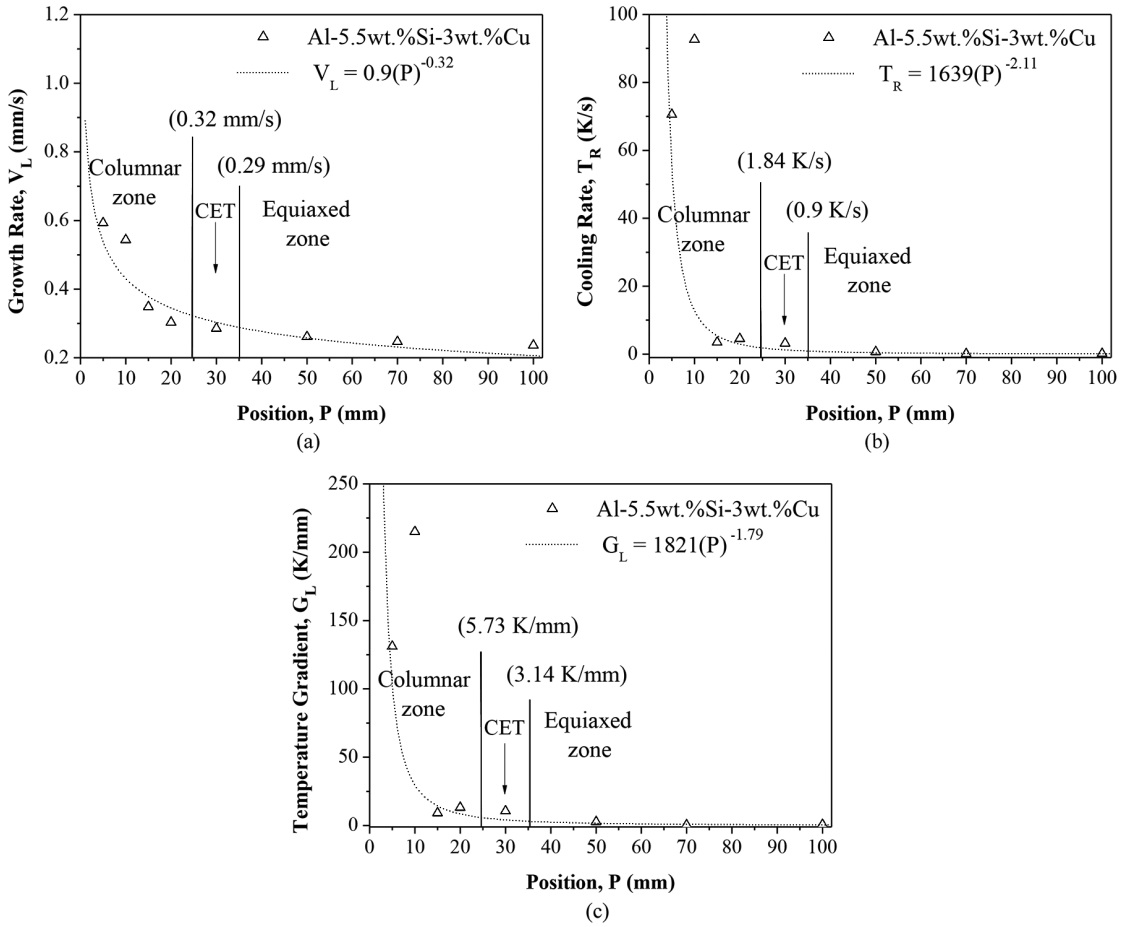


Figure 9. Solidification thermal parameters for Al-3wt.%Cu-5.5wt.%Si alloy with 15% of superheat: (a) $V_L=f(P)$, (b) $T_R=f(P)$ and (c) $G_L=f(P)$.

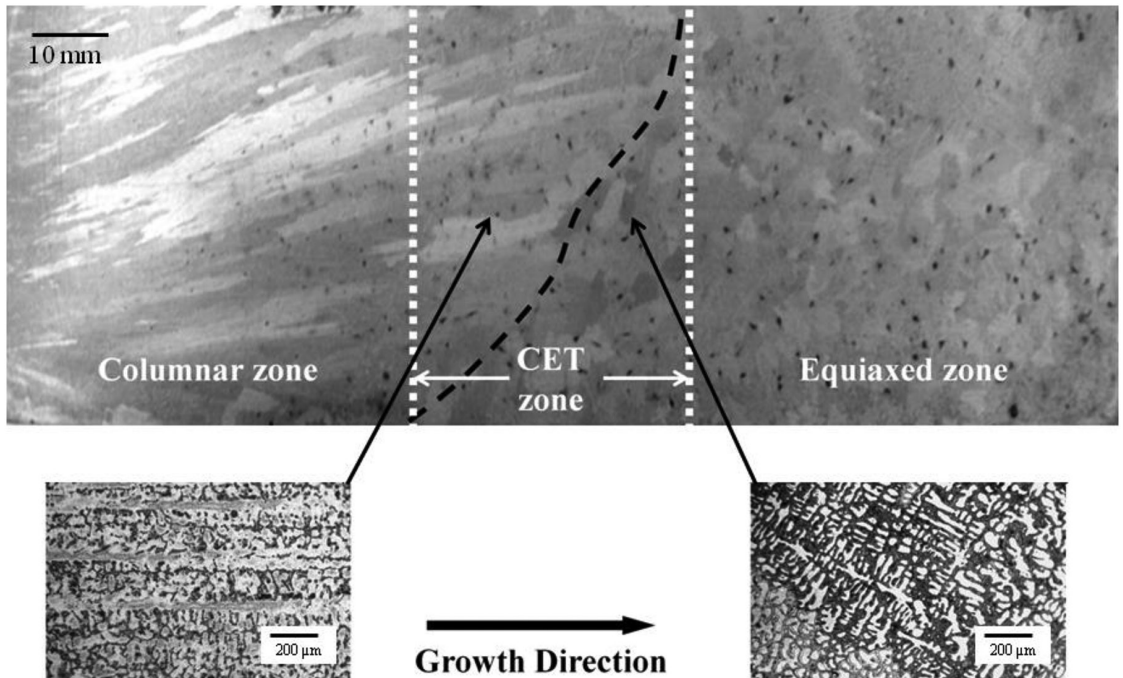


Figure 10. Solidification macrostructure of Al-3.0wt.%Cu-5.5wt.%Si alloy for 5% of superheat, showing CET region in microstructural scale.

Table 4. Experimental results for the solidification thermal parameters associated to the CET zone.

Properties	Superheat	CET zone	Growth rate	Cooling rate	Temperature gradient
Symbols / units	ΔT_v [%]	[mm]	V_L [mm/s]	T_R [K/s]	G_L [K/mm]
Al-3wt.%Cu-5.5wt.%Si	5	55-95	0.8-0.72	5.08-2.73	6.29-3.76
	10	35-70	0.29-0.23	0.9-0.2	3.14-0.91
	15	25-35	0.32-0.29	1.84-0.9	5.73-3.14
Al-3wt.%Cu	6	90-125	0.40-0.33	0.72-0.44	1.77-1.34

4. Conclusions

In this study, the columnar to equiaxed transition was investigated during the horizontal directional solidification of Al-3.0wt.%Cu and Al-3.0wt.%Cu-5.5wt.%Si alloys and the following conclusions can be drawn:

1. For both investigated alloys in this work the CET occurs in a zone rather than in a plane parallel to the chill wall, where both columnar and equiaxed grains coexist. It has been observed that in the case of Al-3.0wt.%Cu-5.5wt.%Si alloy the CET decreases with increasing superheat.
2. For both analyzed alloys in this work the CET position has occurred in a range of growth rates, cooling rates and temperature gradients, according to the values shown in Table 4. It can be verified that during the transition higher values of V_L , T_R and G_L were obtained for superheat equal to 5%.
3. The anticipation of CET observed in the Al-Cu-Si alloy for higher superheats can be assumed by the

combined action of melt thermal and mechanical convection, caused by superheat and solute movements (Si and Cu) at the solidification front contributing, respectively, to the fragmentation of the columnar dendritic branches and at the same time, promoting the dissipation of superheat, increasing the survival of these branches and decreasing the length of the columnar zone.

4. The addition of Si alloying element in the Al-3.0wt.%Cu alloy to form the Al-3.0wt.%Cu-5.5wt.%Si alloy seems to have favored the CET.

Acknowledgements

The authors acknowledge the financial support provided by IFPA (Federal Institute of Education, Science and Technology of Pará), UFPA (Federal University of Pará), CAPES (Coordination of Superior Level Staff Improvement) and CNPq (The Brazilian Research Council- Brazil).

References

1. Peres MD, Siqueira CA and Garcia A. Macrostructural and microstructural development in Al-Si alloys directionally solidified under unsteady-state conditions. *Journal of Alloys and Compounds*. 2004; 381(1-2):168-181. <http://dx.doi.org/10.1016/j.jallcom.2004.03.107>.
2. Siqueira CA, Cheung N and Garcia A. The columnar to equiaxed transition during solidification of Sn-Pb alloys. *Journal of Alloys and Compounds*. 2003; 351(1-2):126-134. [http://dx.doi.org/10.1016/S0925-8388\(02\)01026-5](http://dx.doi.org/10.1016/S0925-8388(02)01026-5).
3. Siqueira CA, Cheung N and Garcia A. Solidification thermal parameters affecting the columnar-to-equiaxed transition. *Metallurgical and Materials Transactions. A, Physical Metallurgy and Materials Science*. 2002; 33A(7):2107-2118. <http://dx.doi.org/10.1007/s11661-002-0042-4>.
4. Canté MV, Cruz KS, Spinelli JE, Cheung N and Garcia A. Experimental analysis of the columnar-to-equiaxed transition in directionally solidified Al-Ni and Al-Sn alloys. *Materials Letters*. 2007; 61(11-12):2135-2138. <http://dx.doi.org/10.1016/j.matlet.2006.08.032>.
5. Spinelli JE, Ferreira IL and Garcia A. Influence of melt convection on the columnar to equiaxed transition and microstructure of downward unsteady-state directionally solidified Sn-Pb alloys. *Journal of Alloys and Compounds*. 2004; 384(1-2):217-226. <http://dx.doi.org/10.1016/j.jallcom.2004.04.098>.
6. Martorano MA and Biscuola VB. Predicting the columnar-to-equiaxed transition for a distribution of nucleation undercoolings. *Acta Materialia*. 2009; 57(2):607-615. <http://dx.doi.org/10.1016/j.actamat.2008.10.001>.
7. Carvalho DB, Moreira AL, Moutinho DJ, Filho JM, Rocha OL and Spinelli JE. The columnar to equiaxed transition of horizontal unsteady-state directionally solidified Al-Si alloys. *Materials Research*. 2013; 17(2):498-510. <http://dx.doi.org/10.1590/S1516-14392014005000015>.
8. Silva JN, Moutinho DJ, Moreira AL, Ferreira IL and Rocha OL. The columnar to equiaxed transition during the horizontal directional solidification of Sn-Pb alloys. *Journal of Alloys and Compounds*. 2009; 478(1-2):358-366. <http://dx.doi.org/10.1016/j.jallcom.2008.11.026>.
9. Ares AE, Gueijman SF and Schvezov CE. An experimental investigation of the columnar-to-equiaxed grain transition in aluminum-copper hypoeutectic and eutectic alloys. *Journal of Crystal Growth*. 2010; 312(14):2154-2170. <http://dx.doi.org/10.1016/j.jcrysgro.2010.04.040>.
10. Badillo A and Beckermann C. Phase-field simulation of the columnar-to-equiaxed transition in alloy solidification. *Acta Materialia*. 2006; 54(8):2015-2026. <http://dx.doi.org/10.1016/j.actamat.2005.12.025>.
11. Doherty RD, Cooper PD, Bradbury MH and Honey FJ. On the columnar-to-equiaxed transition in small ingots. *Metallurgical Transactions. A, Physical Metallurgy and Materials Science*. 1977; 8(3):397-402. <http://dx.doi.org/10.1007/BF02661748>.
12. Wu M, Fjeld A and Ludwig A. Modelling mixed columnar-equiaxed solidification with melt convection and grain sedimentation-Part

- I: model description. *Computational Materials Science*. 2010; 50(1):32-42. <http://dx.doi.org/10.1016/j.commatsci.2010.07.005>.
13. Wu M, Ludwig A and Fjeld A. Modelling mixed columnar-equiaxed solidification with melt convection and grain sedimentation-Part II: illustrative modeling results and parameter studies. *Computational Materials Science*. 2010; 50(1):43-58. <http://dx.doi.org/10.1016/j.commatsci.2010.07.006>.
 14. Wang FY and Beckermann C. Prediction of columnar-to-equiaxed transition during diffusion-controlled dendritic alloy solidification. *Metallurgical and Materials Transactions. A, Physical Metallurgy and Materials Science*. 1994; 25(5):1081-1093. <http://dx.doi.org/10.1007/BF02652282>.
 15. Flood SC and Hunt JD. Columnar and equiaxed growth: I. A model of a columnar front with a temperature dependent velocity. *Journal of Crystal Growth*. 1987; 82(3):543-551. [http://dx.doi.org/10.1016/0022-0248\(87\)90346-0](http://dx.doi.org/10.1016/0022-0248(87)90346-0).
 16. Hunt JD. Steady state columnar and equiaxed growth of dendrites and eutectic. *Materials Science and Engineering*. 1984; 65(1):75-83. [http://dx.doi.org/10.1016/0025-5416\(84\)90201-5](http://dx.doi.org/10.1016/0025-5416(84)90201-5).
 17. Rocha OL, Gomes LG, Moutinho DJ, Ferreira IL and Garcia A. The columnar to equiaxed transition in the directional solidification of aluminum based multicomponent alloys. *Revista Escola de Minas*. 2015; 68(1):85-90. <http://dx.doi.org/10.1590/0370-44672015680237>.
 18. Mahapatra RB and Weinberg F. The columnar to equiaxed transition in tin-lead alloys. *Metallurgical Transactions. B, Process Metallurgy*. 1987; 18(2):425-432. <http://dx.doi.org/10.1007/BF02656163>.
 19. Ziv I and Weinberg F. The columnar-to-equiaxed transition in Al 3Pct Cu. *Metallurgical Transactions. B, Process Metallurgy*. 1989; 20(5):731-734. <http://dx.doi.org/10.1007/BF02655931>.
 20. Suri VK, El-Kaddah N and Berry JT. Control of macrostructure in aluminum casting, part I: determination of columnar/equiaxed transition for Al-4.5%Cu alloy. *AFS Transactions*. 1991; 187:191.
 21. Ares AE and Schvezov CE. Solidification parameters during the columnar-to- equiaxed transition in lead-tin alloys. *Metallurgical and Materials Transactions. A, Physical Metallurgy and Materials Science*. 2000; 31(6):1611-1625. <http://dx.doi.org/10.1007/s11661-000-0171-6>.
 22. Rocha OL, Siqueira CA and Garcia A. Heat flow parameters affecting dendrite spacings during unsteady-state solidification of Sn-Pb and Al-Cu alloys. *Metallurgical and Materials Transactions. A, Physical Metallurgy and Materials Science*. 2003; 34(4):995-1006. <http://dx.doi.org/10.1007/s11661-003-0229-3>.